Multi-disciplinary geoscientific expedition to Woodfjorden, NW Svalbard: Field sites, methods, and preliminary results

Kim Senger[1,2,*], Peter Betlem[1,3], Anniken Helland-Hansen[4], Rafael Kenji Horota[1,5], Horst Kämpf[6], Agnes Kontny[7], Alexander Minakov[3], Sverre Planke[3,8], Sebastian Tappe[4], Maria Telmon[4], Dmitrii Zastrozhnov[3]

[1]*Department of Arctic Geology, The University Centre in Svalbard, PO Box 156, 9171 Longyearbyen, Norway*
[2]*Geodynamics of the Polar Regions, Department of Geosciences, University of Bremen, Klagenfurter Str. 2, 28359, Bremen, Germany*
[3]*Department of Geosciences, University of Oslo, P.O. Box 1047 Blindern, 0316 Oslo, Norway*
[4]*Department of Geosciences, UiT - The Arctic University of Norway, Dramsveien 201, Tromsø, Norway*
[5]*Department of Earth Science, University of Bergen, Allegaten 41, 5020, Bergen, Norway*
[6]*GeoForschungsZentrum (GFZ; German Research Center for Geosciences), Telegrafenberg, 14473 Potsdam, Germany*
[7]*Institute of Applied Geosciences, Karlsruhe Institute of Technology, Adenauerring 20a, 76131 Karlsruhe, Germany*
[8]*Volcanic Basin Energy Research (VBER), Høienhald, Blindernveien 5, 0361 Oslo, Norway*

DOI: 10.5817/CPR2023-2-12

Key words: High Arctic, volcanism, basalt, peridotite xenoliths, hydrothermal fluids, digitalization, Svalbard

---

Received October 3, 2023, *accepted* December 17, 2023.
[*]Corresponding author: K. Senger <kims@unis.no>
Acknowledgements: The expedition was jointly funded by the Research Council of Norway (RCN; Svalbard Strategic Project Svalbox 2.0, several Arctic Field Grant projects, DYPOLE/325984, PALMAR/336293, PHAB Centre of Excellence), the University of the Arctic (Svalbox2020 project), UiT - The Arctic University of Norway, the German Research Foundation (DFG 530455879), and the PALMAR, PDRILL, and NOR-R-AM research projects (UiO). UNIS logistics department provided vital field equipment and safety training. We thank Maxim Smirnov (Luleå University of Technology, LTU) for kindly lending the MT equipment and his technical assistance. The Governor of Svalbard granted permissions to carry out the MT and other sampling work (RIS ID 122222), including a brief visit by selected scientists (Kämpf, Senger, Tappe) to the highly restricted area around Trollkjeldene. Aleksandra Smyrak-Sikora is thanked for feedback on this manuscript. All expedition members sincerely thank the captain and crew of Ulla Rinman for the provision of a safe and enjoyable 'base camp at sea'. Our field program would not have been possible without the strong commitment of the team of Ulla Rinman.

Abstract

The Woodfjorden area of northern Spitsbergen (NW Svalbard) offers access to the world's northernmost onshore thermal springs, extinct Pleistocene alkali basaltic volcanoes and Miocene flood basalts including extensive hyaloclastites. In July 2023, we undertook a 14-day international multi-disciplinary geoscientific expedition to Woodfjorden-Bockfjorden to investigate the Cenozoic geological evolution of the area. The expedition objectives spanned a wide range of scientific topics from sampling of fluids and gas in the thermal springs to constraining the lithosphere by acquiring magnetotelluric data and sampling volcanic rocks. More specifically, we have 1) conducted gas, fluid and travertine sampling at the thermal springs of Gygrekjelda, Jotunkjeldene and Trollkjeldene, 2) mapped and sampled the Quaternary volcanic centers at Sverrefjellet and Halvdanpiggen, 3) sampled the Miocene basalts of the Seidfjellet Formation along seven profiles plus the underlying Devonian sedimentary rocks, 4) acquired magnetotelluric data at 12 stations along both coasts of Woodfjorden and Bockfjorden and 5) collected extensive digital geological data (digital outcrop models and photospheres) using unmanned aerial vehicles (UAVs; also known as drones). The collected samples are currently being analyzed for, amongst others, petrology, geochemistry and geochronology. In this contribution, we report on the expedition's background, scientific objectives and present selected preliminary results such as field parameters from the thermal springs (temperature, pH, electrical conductivity), magnetic susceptibility of volcanic rocks and digital outcrop models plus photospheres.

Introduction

The Svalbard archipelago comprises 62 700 km^2 of uplifted land that is geologically representative of the submerged Barents Shelf to the south-east. Spectacular rock exposures on Svalbard provide insights into the evolution of the North Atlantic and the Arctic basins. The bedrock of Svalbard is bounded by a steep passive margin towards the Arctic Ocean in the north, a sheared passive margin toward the Greenland Sea to the west, whereas to the south and east it continues into the Barents Shelf (Fig. 1).

Svalbard's Phanerozoic sedimentary succession is largely continuous and reflects regional tectonic settings and changing depositional conditions as Svalbard moved northwards from near-equator latitudes (*e.g.*, Henriksen et al. 2011b, Olaussen et al. 2024, Worsley 2008). However, two major hiatuses are identified (Fig. 2). The first one is related to thermally-induced uplift related to magmatism associated with the High Arctic Large Igneous Province (HALIP, Polteau et al. 2016, Senger and Galland 2022, Senger et al. 2014) and led to erosion of the Upper Cretaceous strata (Smelror and Larssen 2016). The second hiatus is evident in the Neogene when sediments were deposited in the offshore areas west and north of Svalbard (Lasabuda et al. 2021). Neogene uplift has been characterized by several methods as reviewed by Lasabuda et al. (2021). These include borehole compaction trends (Henriksen et al. 2011a), apatite-fission track analysis (Dörr et al. 2013), seismic refraction data analysis from sonobuoys and onshore erosion estimates from re-deposited sediment volumes offshore (Dimakis et al. 1998). Although the highest uplift over the Barents Shelf is in Svalbard, it remains unclear how much lateral variation exists, also in the presence of long-lived lineaments is poorly constrained. Early Quaternary glaciations shaped the present-day landscape of Svalbard (Gjermundsen et al. 2015).

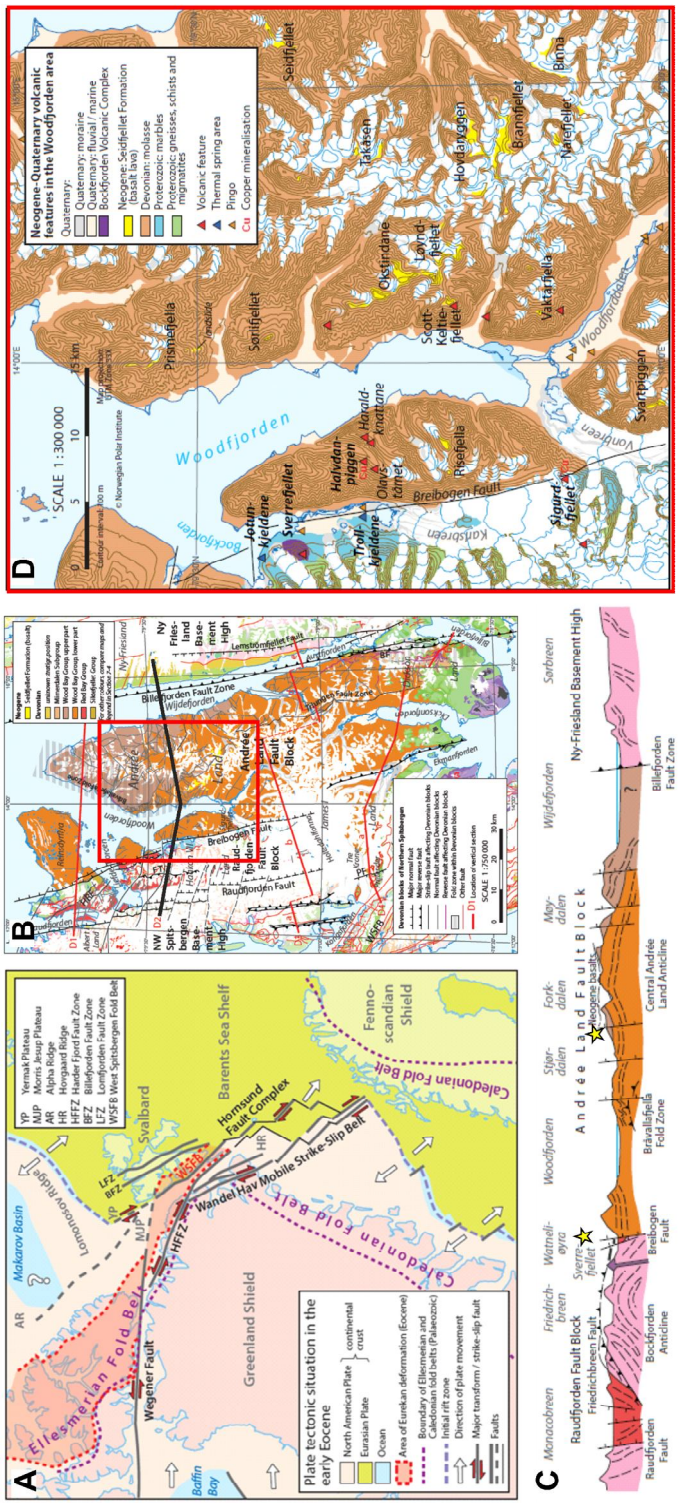

Fig. 1. Geological introduction to the study area. A) Geodynamic setting, illustrated by the situation in the early Eocene. B) Tectonic setting. C) Regional cross-section illustrating the main tectono-thermal elements. D) Geological map. All figure elements are compiled from Dallmann (2015).

There is ongoing surface uplift, as evidenced by several GNSS stations in Svalbard. At the Ny Ålesund station, which is closest to Woodfjorden, the uplift is measured at a rate of 9.5 mm/year, but only 2.7 mm/year can be attributed to glacio-isostatic adjustments following Holocene glacier fluctuations (Kierulf et al. 2022). The remainder component of the uplift must be related to ongoing tectonism, as indicated by earthquakes and locally enhanced heat flow (Minakov 2018, Senger et al. 2023). Temperature and age estimates from peridotites from the Bockfjorden Volcanic Complex, heat flow measurements and tectonic uplift determination suggest the presence of an old but strongly thinned lithospheric mantle root beneath Svalbard (Choi et al. 2010, Vågnes and Amundsen 1993). An in-depth understanding of the interlinkage between mantle and surface processes on a regional scale, particularly in the presence of long-lived tectonic lineaments, is crucial to accurately constrain the controlling mechanisms governing the late Cenozoic evolution of Svalbard.

The remote Woodfjorden area of northern Spitsbergen with its extinct Neogene-Quaternary volcanism provides important information about the geodynamic evolution of the Arctic Basin. Furthermore, the area hosts the world's northernmost onshore thermal springs (Fig. 1D) that indicate a locally enhanced geothermal gradient. From 17th to 31st July 2023 an international multi-disciplinary geoscientific expedition has worked in Woodfjorden to address the following objectives:

- Acquire high-resolution georeferenced digital outcrop models and photospheres of key sites, with emphasis on magma emplacement features.
- Mapping of volcanic-related deposits of the Pleistocene Bockfjorden Volcanic Complex and the Miocene Seidfjellet Formation.
- Systematic sampling of the basaltic rocks and entrained mantle-derived xenoliths for petrological, geochemical, and geochronological analyses.
- Systematic sampling of the water, gas, and travertine deposits from the thermal springs.
- Conduct a magnetotelluric survey to investigate the electrical conductivity structure of the upper crust.

In this contribution we primarily report on the expedition's outcome in terms of new scientific material from this remote area in the High Arctic. We present some preliminary results from the multi-disciplinary research, including field parameters (temperature, pH and electrical conductivity of thermal springs), magnetic susceptibility data for volcanic rocks and digital outcrop models.

Geological setting of the Woodfjorden area

The Woodfjorden area is located about 200 km east of the NE Atlantic-Arctic Mid Ocean Ridge system and part of the European-Eurasian continent-ocean boundary system. The Cenozoic evolution of the area has been debated for decades with various interpretations put forward by, for instance, Vågnes and Amundsen (1993), Dörr et al. (2013), Minakov (2018), Farnsworth et al. (2020) and Dumais et al. (2022).

The scientific target area in northern Spitsbergen comprises Woodfjorden and its sidearm, Bockfjorden (Fig. 1). A major north-south trending fault zone, the Breibogen Fault, separates Devonian rocks to the east from Mesoproterozoic basement rocks to the west. Three Pleistocene volcanic centers lie directly on or immediately adjacent to the Breibogen Fault. Thick basaltic lava flows of the Miocene Seidfjellet Formation unconformably overlie the variably folded and tilted Devonian sedimentary rocks.

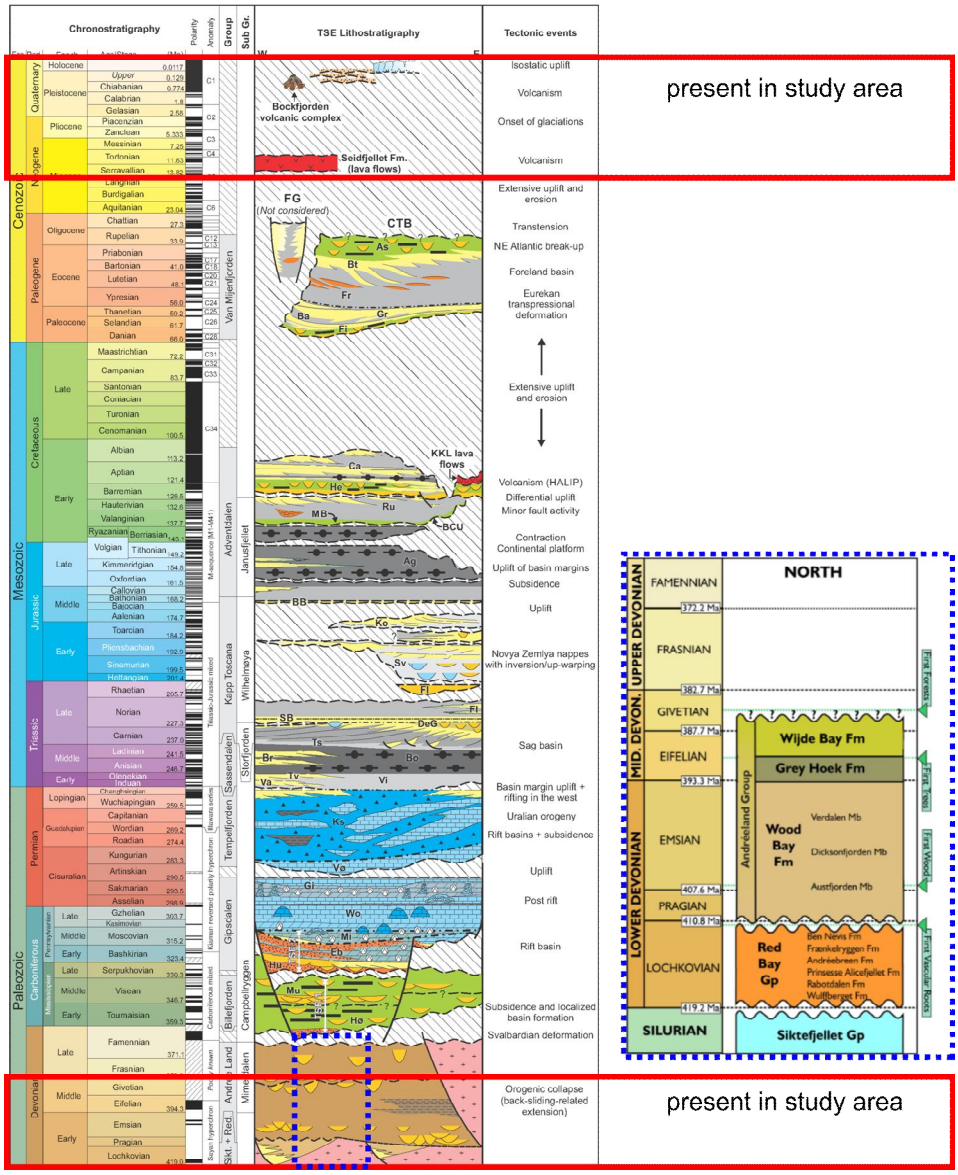

Fig. 2. Regional stratigraphic column, adapted from Olaussen et al. (2024) highlighting the main tectono-thermal events affecting Svalbard since the Devonian. The Seidfjellet Formation unconformably overlies Devonian sedimentary rocks in the study area. The Devonian chronostratigraphic chart is adapted from Davies et al. (2021), with coverage highlighted by the blue dashed box.

Tectonic and stratigraphic setting

The study area exposes Devonian rocks to the east of the Breibogen Fault and Mesoproterozoic marbles and gneisses to the west. These units are locally covered by Miocene and Quaternary basaltic volcanic rocks of the Seidfjellet Formation and the Bockfjorden Volcanic Complex, respectively. The Devonian terrestrial sandstone-siltstone-shale successions were deposited in large fault-bounded basins following the collapse of the Caledonian mountain chain. The early to middle Devonian rocks are affected by the compressional late Devonian Bråvallafjella Fold Zone (Svalbardian event, Ellesmerian orogeny; Dallmann 2015). The Devonian succession and pre-Devonian basement of Svalbard, was tilted southwards during the Early Cretaceous, caused by the opening of the Amerasian Basin and the emplacement of the High Arctic Large Igneous Province (Senger et al. 2014).

Seidfjellet Formation

The Seidfjellet Formation was formally defined by Dallmann et al. (1999) based largely on work by Prestvik (1978). It comprises Miocene basalts (K-Ar and Ar/Ar dating; 11.5 ± 1.2 Ma and 10.4 ± 1.1 Ma; Burov and Zagruzina 1976, Prestvik 1978) that overlie the Devonian sedimentary rocks and infill the paleotopography. Locally the up to 15 preserved basalt lava flows exceed 400 m in cumulative thickness, with 275 m preserved thickness at the type section on Seidfjellet mountain near Wijdefjorden (Dallmann et al. 1999). Geochemically, both tholeiitic and alkaline compositions have been reported based on a very small set of samples (Prestvik 1978), but this apparent dichotomy requires further new investigations of the basalt magma geochemistry. Seidfjellet Formation magmatism was probably more widespread than suggested by the limited distribution of volcanic rock exposures at present, as supported by the recently discovered Middle Miocene basaltic rocks from the offshore Sophia Basin north of Svalbard (Geissler et al. 2019). Figure 3A illustrates some of the exposures of the Seidfjellet Formation.

Bockfjorden Volcanic Complex

Three main volcanic centers comprise the Bockfjorden Volcanic Complex (BVC), namely Sverrefjellet (Fig. 3B), Halvdanpiggen and Sigurdfjellet. These are all located on or near the Breibogen Fault. The BVC was formally defined by Dallmann et al. (1999), based primarily on work by Skjelkvåle et al. (1989). The BVC is particularly well-known for the high abundance of mantle-derived xenoliths such as spinel peridotites (Amundsen et al. 1987, 1988; Choi et al. 2010, Grégoire et al. 2010, Griffin et al. 2012, Skjelkvåle et al. 1989). Calculated equilibration temperatures of these xenoliths allowed for the reconstruction of a lithosphere-scale regional geotherm, which suggests that the crust–mantle boundary is located at approximately 27 km depth (Amundsen et al. 1987). New developments in the field of thermobarometry now enable us to also calculate equilibration pressures for spinel peridotites so that better constraints can be placed on the depth of the lithosphere–asthenosphere boundary beneath northern Spitsbergen. Sverrefjellet volcano was first described scientifically by Gjelsvik (1963) and has more recently been dated to 1.05 ± 0.07 Ma with the bulk-rock $^{40}Ar/^{39}Ar$ technique (Treiman 2012).

Thermal springs

The world's northernmost known onshore thermal springs are reported from the Bockfjorden area, including Trollkjeldene, Jotunkjeldene and Gygrekjelda (Figs. 1D, 3C). The Gygrekjelda spring approximately 3 km north-east of Jotunkjeldene was only discovered in 1995 (Salvigsen and Høgvard 1998). The Jotunkjeldene spring system comprises two thermal springs with travertine terraces, approximately 50 and 60 m in diameter. They are located at the shore of Bockfjorden and thus relatively frequently visited by tourist groups travelling by boat. The Trollkjeldene springs include six individual travertine complexes aligned along the Breibogen Fault. Measured water temperatures range between 19.0°C and 28.3°C (Dallmann 2015).

According to Banks et al. (1998) the Na, K, Si and SO_4 content of the Bockfjord thermal springs is determined by water-rock equilibrium at which water salinity is influenced mainly by fluid-rock interactions with the Mesoproterozoic marbles. The authors note that the bromide deficit in Cl/Br ratios is not clear (approaches of explanation: partial derivation from halite evaporites, adsorption of bromide on organic matter or palaeo-seawater have had a different Br/Cl ratio from that of today). According to Hammer et al. (2005) the water chemistry of Bockfjorden thermal water is relatively enriched in Na and depleted in Cl relative to seawater. The interpreted trends of hydrochemistry and hydroisotope (H-2, O-18) were interpreted as a result of water-rock interactions modifying the meteoric-seawater mix. Gas is actively bubbling up in certain areas and has the following reported composition: 70% N_2, 25-30% CO_2, 0.8-1.4% He (Jamtveit et al. 2006). The travertine data reflect seasonal fluctuation in temperatures during carbonate mineral growth (Jamtveit et al. 2006). Hammer et al. (2007) generated the first model for travertine dam formation and Jorge-Villar et al. (2007) identified unaltered biosignatures in travertine by Raman spectroscopy.

Expedition objectives and achievements

The 2023 Woodfjorden expedition focused on both reconnaissance and targeted data acquisition to address the research objectives listed in the Introduction. The multidisciplinary nature of the scientific team facilitated complementary filed studies, ranging from deep-seated (*e.g.*, magnetotelluric survey, mantle xenoliths petrology) to a shallower subsurface (*e.g.*, geomorphology, thermal spring compositions) study scope.

The expedition was organized with a boat-based base camp to minimize potential polar bear encounter and the environmental impact of camp sites. Other advantages brought by the boat-based operation were flexible access to field sites based on changing weather conditions as well as the opportunity to recharge electronic equipment, which was essential to this expedition. A Zodiac rubber boat was used as the shuttle between the base camp and the 18 landing sites, catering for up to four independent field parties consisting of 2 to 6 geoscientists each.

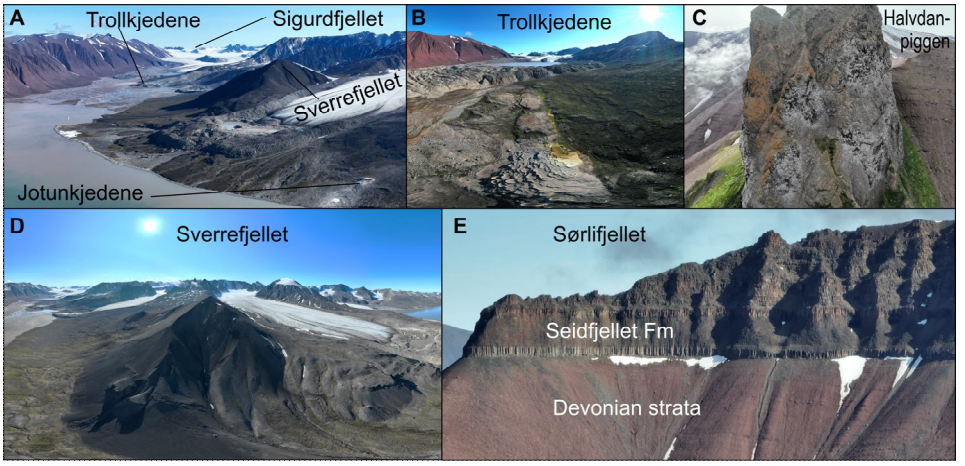

Fig. 3. Photographs taken of selected field sites using unmanned aerial vehicles. A) Overview of the Bockfjorden study area, with the two main thermal springs located on either side of the Sverrefjellet volcano. B) Detailed photograph of the more rarely visited Trollkjedene thermal springs aligned along the Breibogen Fault. C) Circular "neck" of the Halvdanpiggen eruptive center piercing through Devonian sedimentary rocks. D) Photosphere of the Sverrefjellet volcano and its immediate surroundings. Note the Adolfbreen glacier draping the extinct Quaternary volcano. E) Miocene basalt lavas and hyaloclastites of the Seidfjellet Formation emplaced onto the Devonian sedimentary rocks.

Digital geological data acquisition

We used unmanned aerial vehicles (UAVs, *i.e.* drones), namely DJI Mavic 2 Pro and DJI Mavic 3, to collect photographs for generating digital outcrop models and photospheres. In addition, selected pilot sites were digitized at close range (< 4 m) using the in-built LIDAR scanner of an iPhone 12 Pro smartphone. The digital data were integrated in a thematic virtual field trip, freely accessible[1] and illustrated in a video[2].

Photogrammetric digital outcrop modelling

We digitalized 40 key localities and geological exposures as digital outcrop models (DOMs) through photogrammetric processing of UAV-acquired imagery data sets according to standardized protocols using the Agisoft Metashape software (v.2.0.x). Imagery data were collected from close-up (< 50 m) and at longer distances (> 100 m) from the targeted outcrops during manually operated flights. Camera settings and flight operations were optimized to reduce imaging artifacts and facilitate homogeneous illumination of the targets. Specifically, UAV speeds and flight paths were optimized with regards to the camera's shutter speed to avoid motion blur, *i.e.*, considering the time it takes for a point on the ground to move one unit of ground-sampling distance. Other parameters such as lighting conditions, depth of field and image overlap were also considered to improve the suitability of the imagery data for photogrammetric processing. We refer to Betlem et al. (2023) for

further acquisition and processing details. The resulting DOMs show centimetric to decimetric pixel resolutions and are suitable for high-resolution mapping of geological and geomorphological features. Data and metadata will be submitted to the Svalbox Digital Model Database (Betlem et al. 2023; [3]), through which open access to input data, metadata, and processing outputs are guaranteed under the Findable, Accessible, Interoperable, and Reusable (FAIR) principles (Wilkinson et al. 2016). Individual DOMs including input imagery and Metashape projects are continuously being uploaded to the Zenodo repository (*e.g.*, Betlem et al. 2022) with visualization through SketchFab and the Svalbox online portal ([3]; Senger et al. 2020).

Photospheres

Photospheres or 360 images are photo stitched panorama photographs taken around a nodal point. They are commonly used to provide first person view and context of one's surroundings for localization purposes. Photospheres facilitate pre-fieldwork planning and post-field work qualitative analyses. Their rapid and cost-effective acquisition with minimal processing (when compared to quantitative digital outcrop models) make them an important data set for future research, education and outreach activities.

The photospheres taken during the Woodfjorden 2023 expedition were systematically collected over valleys, fjords, and close to outcrops by UAVs. Data and metadata are available through the Svalbox project under FAIR conditions ([3]; Betlem et al. 2023, Senger et al. 2020). In addition, photospheres are combined to build virtual field tours[4] and virtual field guides of key points of interest in the study area for teaching and outreach activities, as illustrated on[5] and discussed by Senger et al. (2021).

Digital field data integration

Access to observations from the field is a key parameter to planning and executing expeditions in remote areas more efficiently. Various tools exist for the documentation of field observations and integration of field data (*e.g.*, FieldMove, Mergin Maps, portable ArcGIS; *e.g.*, Iandelli et al. 2021, Lundmark et al. 2020, Senger and Nordmo 2021), though few facilitate data transfer without an active internet connection. This poses a challenge in off-the-grid areas such as Woodfjorden, and we therefore deployed a self-hosted Mergin Maps (Community Edition, v2023.2) server instance to aid digital field data integration during the expedition. The open-source Mergin Maps provides version-control and local-area-network synchronization that enables simultaneous mapping of localities by different field parties. Regular synchronization provided each team member with up-to-date field projects, including sample lists and field photographs. Integration of Mergin Maps into QGIS further provided a straightforward means to configure the data acquisition templates, as well as for post-expedition data dissemination and visualization (Fig. 4).

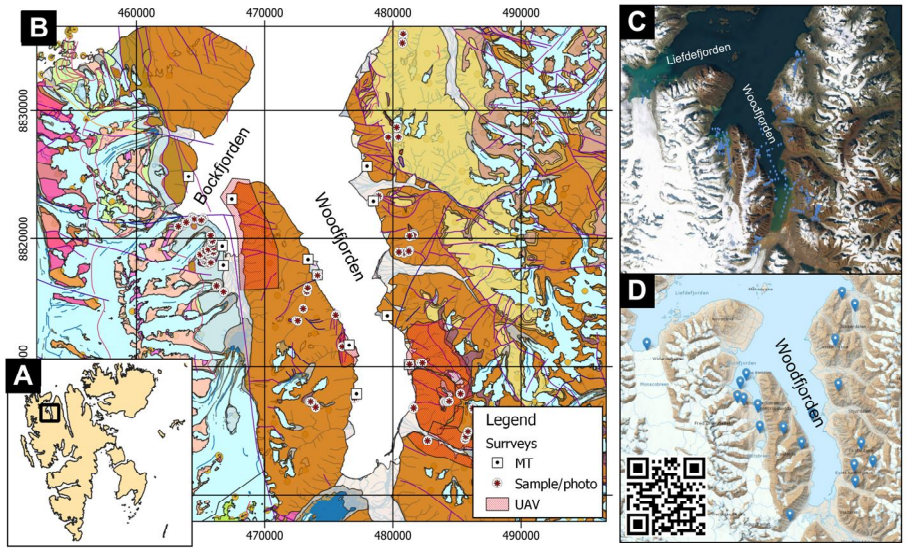

Fig. 4. A) Location of study area in NW Spitsbergen. B) Map generated from the shipboard Mergin Maps project to illustrate spatial coverage of field observations, including MT stations, samples/photo locations and coverage of UAV-flights. C) Location of photospheres in the study area. D) Location of virtual field trips from the study area. Both photospheres and virtual field trips can be accessed via the QR code or the link[6].

Thermal and mineral water springs: water and gas sampling

The study of thermal springs at Trollkjeldene and Jotunkjeldene and the mineral water spring at Gygrekjelda focused on water sampling for hydrochemistry analyses and isotope ratio determinations for hydrogen (H-2, H-3), oxygen (O-18) and chlorine (Cl-36). Besides thermal water samples we also collected sea- and glacial water samples to address the proposed mode of a hydrothermal convection system along the Breibogen Fault feeding the springs. The different water types show a range of field parameters (pH, electrical conductivity, temperature, Table 1). Figure 5 illustrates the temperature and pH of 7 measurements from the thermal and mineral water springs, including the Trollkjeldene, Jotunkjeldene and Gygrekjelda. The second objective was sampling and subsequent laboratory analyses of the free gas phase at the Trollkjeldene and Jotunkjeldene thermal springs (elemental gas composition, C, He, Ne, Ar isotopic compositions). In addition to free gas, we also collected volcanic glass samples from Sverrefjellet and Halvdanpiggen to investigate the elemental compositions and noble gas isotope ratios (He, Ne, Ar) to evaluate if the active gas and the Quaternary magmas are from the same source.

Location	Date of sampling	Water type	pH	T	Conduc-tivity
				°C	mS/cm
coastal, east of Friedrichbreen, Bockfjord	20.7.2023	mixing of sea- and glacial melt water	8.2	8.5	4.06
thermal spring Jotun 1, Bockfjord	20.7.2023	thermal water	6.7	24.4	3.81
lake west of Friedrichbreen, Bockfjord	20.7.2023	glacial melt water	7.81	8	0.0434
thermal spring Gygrekjelda, Bockfjord	20.7.2023	thermal water	7.6	5.1	2.4
Woodfjorden	25.7.2023	sea water	8.33	8.5	43.9
thermal spring Troll D	26.7.2023	thermal water	6.8	26	1.597
thermal spring Troll E, diameter: 11m	26.7.2023	thermal water	6.95	19.1	1.597
thermal spring Troll E, diameter: 3,2m	26.7.2023	thermal water	6.87	20.4	1.928
thermal spring Jotun 1, Bockfjord	27.7.2023	thermal water	6.73	24.4	3.85
Bockfjorden	29.7.2023	sea water	8.38	7.8	45.2
Liefdefjorden	29.7.2023	sea water	8.36	7	42.8

Table 1. Field parameters (temperature, pH and electrical conductivity) of water samples, collected during the expedition.

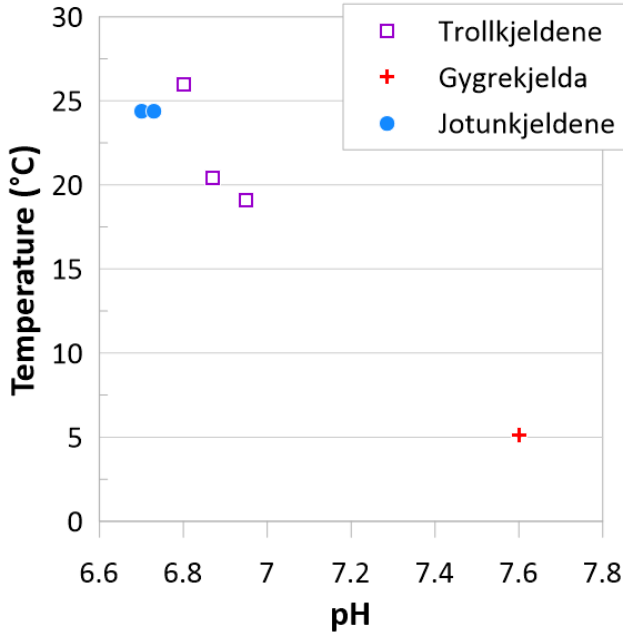

Fig. 5. Field parameters (temperature, pH) of water samples collected from thermal and mineral water springs during the expedition.

Bockfjorden Volcanic Complex: sampling, geomorphology and volcanic facies

The Quaternary BVC consists of three main outcrops: Sverrefjellet, Halvdanpiggen, and Sigurdfjellet. Sverrefjellet is a subglacial volcanic complex, characterized by subaqueous pillow basalts and basaltic lava flows, mingled fractured basalt and volcanogenic sediments, and locally an apron of steeply dipping volcanogenic sediments. World-class outcrops of mantle-derived xenoliths are present in all the units, including the few dykes that were identified in the field (Fig. 6D). In places, undulating zones with platy basalt were documented, both near the base of flow units and at the contacts of steeply dipping dykes. Halvdanpiggen is an impressive cylindrical mountain rising more than a hundred meters above the surrounding eroded Devonian sedimentary rocks (Fig. 3C). It consists of several smaller (~ 10 m in diameter) pipes along its eastern slope and one larger pipe at the top of the mountain, which hosts a bird colony. The outcrop is dominated by intensely fractured and jointed basalt. Mantle xenoliths are common within the pipe, whereas crustal xenoliths dominate one cliff section. The Sigurdfjellet volcano is difficult to access without helicopter support due to deep crevasses in the glacier. Nonetheless, we sampled several xenoliths downslope from Sigurdfjellet.

We will undertake comprehensive geochemical analyses of the acquired samples to characterize the tectono-magmatic evolution of the Bockfjorden Volcanic Complex. A further topic is the investigation of the eruption age of Halvdanpiggen using $^{40}Ar/^{39}Ar$ dating to complement the study by Treiman (2012) on Sverrefjellet.

Seidfjellet Formation: sampling, volcanic architecture and base basalt morphology

During the 2023 expedition to Woodfjorden, the Seidfjellet Formation was systematically sampled (Fig. 6F). The Seidfjellet Formation was emplaced onto Devonian sedimentary rocks incised by river valleys and lakes before the lava outpouring during the Miocene. The main volcanic outcrops are presently located at 800 to 1200 m elevation. Collectively they form the remnants of a Miocene flood basalt province that originally emplaced at much lower but unknown elevation. The up to 350 m thick volcanic pile of more than 15 discrete lava flows accumulated in paleo-depressions on the Miocene peneplain, which had developed on the Devonian bedrock. Post-Miocene uplift and erosion led to the spectacular topography and geological exposures flanking the shores of Woodfjorden. During the 2023 expedition, the peaks of Scott-Keltiefjellet, Lavatoppen, Risefjella, Prismefjella and Prinsetoppen were locally profiled to determine the amount of lava flows present. The use of 3D models from drone surveys will aid to confirm our fieldwork observations. Furthermore, each outcrop profile was systematically sampled for geochronology, petrology and geochemistry research (*e.g.*, high-precision U-Pb CA-ID-TIMS analysis, bulk-rock major and trace element analysis, long- and short-lived radiogenic isotope systems, traditional and nontraditional stable isotopes, noble gas isotopes). The 2023 sample collection will be merged with basalt samples obtained in 2022 during a helicopter survey of the region.

Currently, the nature and location of the igneous plumbing system and eruption centers are poorly constrained by outcrop data because only a few sills and dykes of uncertain age have been observed in the study area. The subhorizontal contact zone between the Devonian sedimentary rocks and Miocene basalts is well exposed in the

Løyndfjellet mountain range, but is covered by scree elsewhere. The initial volcanic deposits vary from volcanogenic sediments, with up to 50 m thick hyaloclastite deposits in the Scott Keltiefjellet area, to up to 30-50 m thick basaltic lava flows with well-developed columnar jointing in the lower massive part and chaotic fracturing in the upper vesicular part. Vesicles are almost always open, and vein mineralization is scarce. The bottom interval of 2 or 3 thickened basaltic lava flows or hyaloclastites is overlain by up to 15 tabular flood basalt units, locally with pahoehoe flow tops. No inter-basalt sediment layers were identified, and overlying sediments are absent.

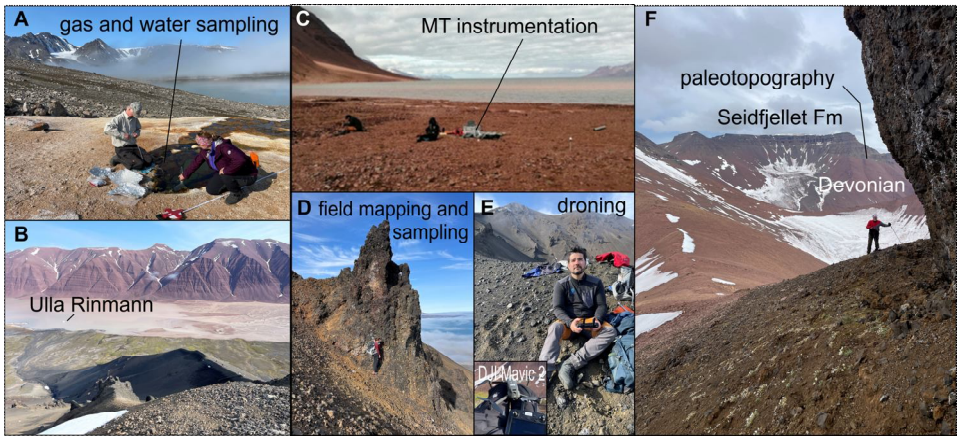

Fig. 6. Compilation of field photos of the multi-disciplinary data acquisition. A) Gas sampling at the Jotunkjeldene thermal springs. B) Overview from the ridge of Sverrefjellet. C) Installation of MT site W05 on the alluvial fan on the western shore of Woodfjorden. D) Geologist studying xenoliths within an outcrop at Sverrefjellet. E) UAV pilot at Sverrefjellet. The inset image shows the Mavic 2 Pro drone with smart controller. F) Overview of the Miocene Seidfjellet Formation overlying Devonian sedimentary rocks at Løyndfjellet. The geologist is examining hyaloclastite deposits on Scott-Keltiefjellet.

Shore profiles at Woodfjorden and altitude profiles at Wood Bay Formation: uplift rate and exhumation rate studies

The amount of Post-Miocene erosion of the volcanic succession is currently unconstrained and one of the research questions to be addressed by our analytical program.

During the expedition in Woodfjorden, we started a pilot study, not planned before, to investigate the uplift rate in the Holocene. We collected drift wood samples and marine biota at 4 profiles, run from sea to coastal terrace(s). Parallel to this the geomorphology team collected photographs at the profiles by UAVs to prepare elevation models. The idea is to determine C-14 ages from wood and marine biota samples and use digital elevation models for the reconstruction of the uplift rate during the last 12.000 years.

In addition, the Lower Devonian Wood Bay Formation was systematically sampled in different localities and altitudes to generate a thermochronology profile based on zircons cooling ages and estimate the exhumation rate of the region.

Magnetic susceptibility and sampling for magnetic petrology

Quaternary volcanic rocks from the Bockfjorden Volcanic Complex (Sverrefjellet, Halvdanpiggen and Sigurdfjellet) were collected in the field and magnetic susceptibility was measured with a hand-held Kappa meter (SM-30). Different volcanic rock types and in some cases also their contact metamorphic aureoles within the host rocks show a range of magnetic susceptibility values (Table 1). In general, the volcanic rocks show ferrimagnetic susceptibilities, with similar average values for the Quaternary BVC (3.76×10^{-3} SI) and Miocene Seidfjellet Formation (4.93×10^{-3} SI). However, there is a significant variation within and between different rock types, especially for the different volcanic rocks from the BVC. Basalts from the Halvdanpiggen pipes show the highest values (14.36×10^{-3} SI), whereas tuff from the Sverrefjellet volcano shows only low, paramagnetic susceptibility (0.38×10^{-3} SI) indicating rapid quenching of the magma during fragmentation, typical for a subglacial emplacement mode (e.g., Oliva-Urcia et al. 2011). The mantle-derived xenoliths are dominantly paramagnetic with values below 0.5×10^{-3} SI, with few exceptions (Table 2). These values agree well with earlier determinations of the magnetic susceptibility by Ladygin et al. (2003). The reasons for these susceptibility variations will be further studied by field- and temperature-dependent magnetic susceptibility along with reflected light microscopy to identify and characterize the magnetic mineralogy of the different volcanic rocks. These data may help to understand the emplacement mechanism of the basaltic volcanic rocks (*e.g.*, subglacial versus subaerial), and help to better constrain titanomagnetite formation in peridotitic mantle rocks.

Magnetotelluric data and electrical conductivity

The crustal structure plays a crucial role in understanding the geological, geochemical, and evolutionary aspects of volcanic areas. The magnetotelluric (MT) method is an effective technique for obtaining primary data on the crustal structure in active and recently extinct (*e.g.*, Neogene) volcanic areas. The resulting electrical resistivity images provide valuable information about deep mineralization, the presence of fluids, and temperature distribution in the subsurface. In Svalbard, several local and semi-regional onshore 2-D MT surveys have been conducted in the past decade (Beka et al. 2017a, b; Beka et al. 2016, Selway et al. 2020), as well as an offshore survey that combined controlled-source electromagnetic-MT profile across the mid-ocean ridge west of Svalbard (Johansen et al. 2019). During our 2023 expedition, we conducted the first semi-regional 3-D MT survey in Woodfjorden to enhance understanding of the crustal structure and fluid distribution. Such data can help to infer the spatial distribution of the Late Cenozoic mantle sourced magmatic system in the upper crust, which is crucial for comprehending the evolution of volcanism in northern Spitsbergen.

We acquired MT data at 12 sites within the Bockfjorden and Woodfjorden area (Fig. 3, Fig. 6C) to obtain the electrical structure of the crust influenced by Miocene and Quaternary mantle sourced volcanic activity. Most of our MT sites were positioned within the Devonian sedimentary basin. Stations W01, W02 and W11 are exceptions because they were placed near Sverrefjellet, which is situated on

Mesoproterozoic basement rocks. The stations were installed mostly on smooth terrain, such as alluvial fans and marine terraces.

For simultaneous data recording, we utilized two broadband MT instruments provided by the Luleå University of Technology (LTU). These instruments were equipped with horizontal coil magnetometers and pairs of LEMI non-polarizing electrodes (Fig. 6C). The time series data of electrical and magnetic fields with a sampling frequency of 20 Hz, and a night burst recording of 1000 Hz was acquired using the EarthData recording unit. The recorded time series of electrical and magnetic fields demonstrates the quality of our data. The collected data were saved in standard miniseed format for subsequent analysis.

In data processing of the above-specified data, we will employ the robust estimation of the magnetotelluric impedance tensor using the multi-variate processing technique by Smirnov and Egbert (2012) for data processing. To map the subsurface electrical conductivity distribution, the impedance tensor data will be inverted using the ModEM 3-D inversion method (Kelbert et al. 2014).

		n	mean	min	max
Bockfjorden Volcanic Complex		***130***	***3.76***	***0.04***	***21.50***
Sverrefjellet	basalt	77	3.24	1.00	11.30
	tuff	8	0.38	0.30	0.46
	mantle xenolith	13	0.66	0.31	2.60
	crustal xenolith	1	0.04	0.04	0.04
Halvdanpiggen	basalt	10	14.36	9.71	21.50
	diatreme breccia	9	4.79	0.34	11.00
Sigurdfjellet	basalt	7	3.41	1.85	4.95
	volcanic breccia	5	2.96	2.47	4.12
Seidfjellet Fm		***50***	***4.93***	***0.72***	***17.80***
	basalt	46	4.83	0.72	17.80
	dyke	4	6.06	4.66	7.08
	contact metamorphic zone in sandstone	3	18.63	11.90	22.10
Devonian	sandstone	17	0.37	0.10	0.80
Proterozoic	gneiss	6	0.20	0.13	0.33

Table 2. Magnetic susceptibility (in 10^{-3} SI units) for rock samples from the Quaternary Bockfjorden Volcanic Complex and Miocene Seidfjellet Formation, as well as selected country rocks (field measurements).

Summary and outlook

In this contribution, we report on a 2-week long geoscientific expedition to the Woodfjorden area of northern Spitsbergen, which took place in July 2023. The multi-disciplinary geosciences team systematically collected data on the geomorphology and geology of the area (digital outcrop models, photospheres, field mapping), collected rock samples from the Bockfjorden Volcanic Complex and the Seidfjellet Formation (for petrological–geochemical and geochronological studies), collected water and gas samples from the world's northernmost onshore thermal springs for subsequent geochemical and isotopic studies, and collected magnetotelluric data across the entire study area for constraining the subsurface electrical conductivity structure. Detailed follow-up studies will be published in the near future, mostly driven by MSc and PhD students as part of their project theses.

References

AMUNDSEN, H., GRIFFIN, W. and O'REILLY, S. Y. (1987): The lower crust and upper mantle beneath northwestern Spitsbergen: evidence from xenoliths and geophysics. *Tectonophysics*, 139(3-4): 169-185. doi: 10.1016/0040-1951(87)90095-3

AMUNDSEN, H., GRIFFIN, W. and O'REILLY, S. Y. (1988): The nature of the lithosphere beneath northwestern Spitsbergen: xenolith evidence. *NGU Special Publication*, (3): 58-65.

BANKS, D., SLETTEN, R. S., HALDORSEN, S., DALE, B., HEIM, M. and SWENSEN, B. (1998): The thermal springs of Bockfjord, Svalbard: Occurrence and major ion hydrochemistry. *Geothermics*, 27(4): 445-467. doi: 10.1016/S0375-6505(98)00022-4

BEKA, T. I., BERGH, S. G., SMIRNOV, M. and BIRKELUND, Y. (2017a): Magnetotelluric signatures of the complex tertiary fold–thrust belt and extensional fault architecture beneath Brøggerhalvøya, Svalbard. *Polar Research*, 36(1): 1409586. doi: 10.1080/17518369.2017.1409586

BEKA, T. I., SENGER, K., AUTIO, U. A., SMIRNOV, M. and BIRKELUND, Y. (2017b): Integrated electromagnetic data investigation of a Mesozoic CO_2 storage target reservoir-cap-rock succession, Svalbard. *Journal of Applied Geophysics*, 136: 417-430, doi: 10.1016/j.jappgeo.2016.11.021

BEKA, T. I., SMIRNOV, M., BIRKELUND, Y., SENGER, K. and BERGH, S. G. (2016): Analysis and 3D inversion of magnetotelluric crooked profile data from central Svalbard for geothermal application. *Tectonophysics*, 686: 98-115. doi: 10.1016/j.tecto.2016.07.024

BETLEM, P., RODES, N., BIRCHALL, T., DAHLIN, A., SMYRAK-SIKORA, A. and SENGER, K. (2023): The Svalbox Digital Model Database: A geoscientific window to the High Arctic. *Geosphere*, 19(6): 1640-1666. doi: 10.1130/GES02606.1

BETLEM, P., RODES, N., HOROTA, R., VAN HAZENDONK, L. and Svalbox team (2022): Svalbox-DOM_2021-0018_Midterhuken. Data set (Zenodo). doi: 10.5281/zenodo.6040362

BUROV, J. P., ZAGRUZINA, V. (1976): Results of a determination of the absolute age of Cenozoic basic rocks of the northern part of the island of Spitsbergen (translated from Russian). *Geologija Sval'barda* (NIIGA, Leningrad): 139-140,

CHOI, S. H., SUZUKI, K., MUKASA, S. B., LEE, J.-I. and JUNG, H. (2010): Lu–Hf and Re–Os systematics of peridotite xenoliths from Spitsbergen, western Svalbard: Implications for mantle–crust coupling. *Earth and Planetary Science Letters*, 297(1): 121-132. doi: 10.1016/j.epsl.2010.06.013

DALLMANN, W. (2015): Geoscience Atlas of Svalbard. *Norsk Polarinstitutt Rapportserie*, 148: 292. http://hdl.handle.net/11250/2580810

DALLMANN, W. K., DYPVIK, H., GJELBERG, J. G., HARLAND, W. B., JOHANNESSEN, E. P., KEILEN, H. B., LARSSEN, G. B., LØNØY, A., MIDBØE, P. S., MØRK, A., NAGY, J., NILSSON, I., NØTTVEDT, A., OLAUSSEN, S., PCELINA, T. M., STEEL, R. J. and WORSLEY, D. (1999): Lithostratigraphic

Lexicon of Svalbard: Review and recommendations for nomenclature use. Norsk Polarinstitutt, Tromsø, 318 p.

DAVIES, N. S., BERRY, C. M., MARSHALL, J. E. A., WELLMAN, C. H. and LINDEMANN, F.-J. (2021): The Devonian landscape factory: Plant–sediment interactions in the Old Red Sandstone of Svalbard and the rise of vegetation as a biogeomorphic agent. *Journal of the Geological Society*, 178(5): jgs2020-225. doi:10.1144/jgs2020-225

DIMAKIS, P., BRAATHEN, B. I., FALEIDE, J. I., ELVERHØI, A. and GUDLAUGSSON, S. T. (1998): Cenozoic erosion and the preglacial uplift of the Svalbard–Barents Sea region. *Tectonophysics*, 300(1–4): 311-327. doi: 10.1016/s0040-1951(98)00245-5

DUMAIS, M. A., GERNIGON, L., OLESEN, O., LIM, A., JOHANSEN, S. and BRÖNNER, M. (2022): Crustal and Thermal Heterogeneities across the Fram Strait and the Svalbard Margin. *Tectonics*, 41(10): e2022TC007302. doi: 10.1029/2022TC007302

DÖRR, N., CLIFT, P. D., LISKER, F. and SPIEGEL, C. (2013): Why is Svalbard an island? Evidence for two-stage uplift, magmatic underplating, and mantle thermal anomalies. *Tectonics*, 32(3): 473-486. doi: 10.1002/tect.20039

FARNSWORTH, W. R., BLAKE JR., W., GUDMUNDSDOTTIR, E. R., INGÓLFSSON, Ó., KALLIOKOSKI, M. H., LARSEN, G., NEWTON, A. J., ÓLADÓTTIR, B. A. and SCHOMACKER, A. (2020): Ocean-rafted pumice constrains postglacial relative sea-level and supports Holocene ice cap survival. *Quaternary Science Reviews*, 250. doi: 10.1016/j.quascirev.2020.106654

GEISSLER, W. H., ESTRADA, S., RIEFSTAHL, F., O'CONNOR, J. M., SPIEGEL, C., VAN DEN BOOGARD, P. and KLÜGEL, A. (2019): Middle Miocene magmatic activity in the Sophia Basin, Arctic Ocean – evidence from dredged basalt at the flanks of Mosby Seamount. *Arktos*, 5(1): 31-48. doi: 10.1007/s41063-019-00066-8

GJELSVIK, T. (1963): Remarks on the structure and composition of the Sverrefjellet volcano, Bockfjorden, Vestspitsbergen. Norsk Polarinstitutt Årbok 1962: 50-54.

GJERMUNDSEN, E. F., BRINER, J. P., AKÇAR, N., FOROS, J., KUBIK, P. W., SALVIGSEN, O. and HORMES, A. (2015): Minimal erosion of Arctic alpine topography during late Quaternary glaciation. *Nature Geoscience*, 8(10): 789-792. doi: 10.1038/ngeo2524

GRÉGOIRE, M., CHEVET, J. and MAALOE, S. (2010): Composite xenoliths from Spitsbergen: evidence of the circulation of MORB-related melts within the upper mantle. Geological Society, London, Special Publications, 337(1): 71-86. doi: 10.1144/SP337.4

GRIFFIN, W. L., NIKOLIC, N., O'REILLY, S. Y. and Pearson, N. J. (2012): Coupling, decoupling and metasomatism: Evolution of crust–mantle relationships beneath NW Spitsbergen. *Lithos*, 149: 115-135. doi: 10.1016/j.lithos.2012.03.003

HAMMER, Ø., DYSTHE, D. K. and JAMTVEIT, B. (2007): The dynamics of travertine dams. *Earth and Planetary Science Letters*, 256(1): 258-263. doi: 10.1016/j.epsl.2007.01.033

HAMMER, Ø., JAMTVEIT, B., BENNING, L. G. and DYSTHE, D. K. (2005): Evolution of fluid chemistry during travertine formation in the Troll thermal springs, Svalbard, Norway. *Geofluids*, 5(2): 140-150. doi: 10.1111/j.1468-8123.2005.00109.x

HENRIKSEN, E., BJØRNSETH, H. M., HALS, T. K., HEIDE, T., KIRYUKHINA, T., KLØVJAN, O. S., LARSSEN, G. B., RYSETH, A. E., RØNNING, K., SOLLID, K. and STOUPAKOVA, A. (2011a): Chapter 17: Uplift and erosion of the greater Barents Sea: impact on prospectivity and petroleum systems. *In*: A. M. Spencer, A. F. Embry, D. L. Gautier, A. V. Stoupakova and K. Sørensen (Eds.): Arctic Petroleum Geology. The Geological Society, London, pp. 271–281. doi: 10.1144/m35.17

HENRIKSEN, E., RYSETH, A. E., LARSSEN, G. B., HEIDE, T., RØNNING, K., SOLLID, K. and STOUPAKOVA, A.V. (2011b): Chapter 10: Tectonostratigraphy of the greater Barents Sea: implications for petroleum systems. *In*: A. M. Spencer, A. F. Embry, D. L. Gautier, A. V. Stoupakova and K. Sørensen (Eds.): Arctic Petroleum Geology. The Geological Society, London, pp. 163–195. doi: 10.1144/m35.10

IANDELLI, N., COLI, M., DONIGAGLIA, T. and CIUFFREDA, A. L. (2021): An unconventional field mapping application: A complete opensource workflow solution applied to lithological mapping of the coatings of cultural heritage. *ISPRS International Journal of Geo-Information*, 10(6): 357. doi: 10.3390/ijgi10060357

JAMTVEIT, B., HAMMER, Ø., ANDERSSON, C., DYSTHE, D., HELDMANN, J. and FOGEL, M. L. (2006): Travertines from the Troll thermal springs, Svalbard. *Norwegian Journal of Geology/Norsk Geologisk Forening*, 86(4). https://njg.geologi.no/images/NJG_articles/B_Jamtveit_et_al.pdf

JOHANSEN, S.E., PANZNER, M., MITTET, R., AMUNDSEN, H.E.F., LIM, A., VIK, E., LANDRØ, M. and ARNTSEN, B. (2019): Deep electrical imaging of the ultraslow-spreading Mohns Ridge. *Nature*, 567(7748): 379-383. doi: 10.1038/s41586-019-1010-0

JORGE-VILLAR, S. E., BENNING, L. G., EDWARDS, H. G. M. and AMASE team (2007): Raman and SEM analysis of a biocolonised hot spring travertine terrace in Svalbard, Norway. *Geochemical Transactions*, 8(1): 8. doi: 10.1186/1467-4866-8-8

KELBERT, A., MEQBEL, N., EGBERT, G. D. and TANDON, K. (2014): ModEM: A modular system for inversion of electromagnetic geophysical data. *Computers & Geosciences*, 66: 40-53. doi: 10.1016/j.cageo.2014.01.010

KIERULF, H. P., KOHLER, J., BOY, J.-P., GEYMAN, E. C., MÉMIN, A., OMANG, O. C., STEFFEN, H. and STEFFEN, R. (2022): Time-varying uplift in Svalbard–an effect of glacial changes. *Geophysical Journal International*, 231(3): 1518-1534. doi: 10.1093/gji/ggac264

LADYGIN, V., FROLOVA, J. V. and GENSHAFT, Y. S. (2003): Petrophysical properties of Quaternary lavas of Spitsbergen. *Russian Journal of Earth Sciences*, 5(4): 291-298.

LASABUDA, A. P. E., JOHANSEN, N. J. S., LABERG, J. S., FALEIDE, J. I., SENGER, K., RYDNINGEN, T. A., PATTON, H., KNUTSEN, S.-M. and HANSSEN, A. (2021): Cenozoic uplift and erosion of the Norwegian Barents Shelf – A review. *Earth-Science Reviews*, 217: 1-35. doi: 10.1016/j.earscirev.2021.103609

LUNDMARK, A.M., AUGLAND, L.E. and JØRGENSEN, S.V. (2020): Digital fieldwork with Fieldmove - how do digital tools influence geoscience students' learning experience in the field? *Journal of Geography in Higher Education*: 1-14. doi: 10.1080/03098265.2020.1712685

MINAKOV, A. (2018): Late Cenozoic lithosphere dynamics in Svalbard: Interplay of glaciation, seafloor spreading and mantle convection. *Journal of Geodynamics*, 122: 1-16. doi: 10.1016/j.jog.2018.09.009

OLAUSSEN, S., GRUNDVÅG, S.-A., SENGER, K., ANELL, I., BETLEM, P., BIRCHALL, T., BRAATHEN, A., DALLMANN, W., JOCHMANN, M., JOHANNESSEN, E. P., LORD, G., MØRK, A., OSMUNDSEN, P. T., SMYRAK-SIKORA, A. and STEMMERIK, L. (2024): Svalbard Composite Tectono-Sedimentary Element, Barents Sea. *Geological Society, London, Memoirs*, 57(1): M57-2021-36. doi: 10.1144/M57-2021-36

OLIVA-URCIA, B., KONTNY, A., VAHLE, C. and SCHLEICHER, A. M. (2011): Modification of the magnetic mineralogy in basalts due to fluid–rock interactions in a high-temperature geothermal system (Krafla, Iceland). *Geophysical Journal International*, 186(1): 155-174. doi: 10.1111/j.1365-246X.2011.05029.x

POLTEAU, S., HENDRIKS, B. W. H., PLANKE, S., GANERØD, M., CORFU, F., FALEIDE, J. I., MIDTKANDAL, I., SVENSEN, H. S. and MYKLEBUST, R. (2016): The Early Cretaceous Barents Sea Sill Complex: Distribution, 40Ar/39Ar geochronology, and implications for carbon gas formation. *Palaeogeography, Palaeoclimatology, Palaeoecology*, 441: 83-95. doi: 10.1016/j.palaeo.2015.07.007

PRESTVIK, T. (1978): Cenozoic plateau lavas of Spitsbergen – a geochemical study. Norsk Polarinstitutt Årbok 1977: 129-143.

SALVIGSEN, O., HØGVARD, K. (1998): Gygrekjelda, a new warm spring in Bockfjorden, Svalbard. *Polar Research*, 17(1): 107-109. doi: 10.3402/polar.v17i1.6613

SELWAY, K., SMIRNOV, M., BEKA, T., O'DONNELL, J. P., MINAKOV, A., SENGER, K., FALEIDE, J. I. and KALSCHEUER, T. (2020): Magnetotelluric constraints on the temperature, composition, partial melt content, and viscosity of the upper mantle beneath Svalbard. *Geochemistry Geophysics Geosystems*, 21(5): 12. doi: 10.1029/2020GC008985

SENGER, K., BETLEM, P., BIRCHALL, T., BUCKLEY, S. J., COAKLEY, B., EIDE, C. H., FLAIG, P. P., FORIEN, M., GALLAND, O., GONZAGA, L., JENSEN, M., KURZ, T., LECOMTE, I., MAIR, K., MALM, R. H., MULROONEY, M., NAUMANN, N., NORDMO, I., NOLDE, N., OGATA, K., RABBEL, O., SCHAAF, N. W. and SMYRAK-SIKORA, A. (2020): Using digital outcrops to make the high Arctic

more accessible through the Svalbox database. *Journal of Geoscience Education*, 69(2): 123-137. doi: 10.1080/10899995.2020.1813865

SENGER, K., BETLEM, P., GRUNDVÅG, S.-A., HOROTA, R.K., BUCKLEY, S.J., SMYRAK-SIKORA, A., JOCHMANN, M.M., BIRCHALL, T., JANOCHA, J., OGATA, K., KUCKERO, L., JOHANNESSEN, R.M., LECOMTE, I., COHEN, S.M. and OLAUSSEN, S. (2021): Teaching with digital geology in the high Arctic: opportunities and challenges. *Geoscience Communication*, 4: 399-420. doi: 10.5194/gc-4-399-2021

SENGER, K., GALLAND, O. (2022): Stratigraphic and Spatial extent of HALIP Magmatism in central Spitsbergen. *Geochemistry, Geophysics, Geosystems*: e2021GC010300. doi: 10.1029/2021GC010300

SENGER, K., NORDMO, I. (2021): Using digital field notebooks in geoscientific learning in polar environments. *Journal of Geoscience Education*, 69(2): 166-177. doi: 10.1080/10899995.2020.1725407

SENGER, K., NUUS, M., BALLING, N., BETLEM, P., BIRCHALL, T., CHRISTIANSEN, H. H., ELVEBAKK, H., FUCHS, S., JOCHMANN, M., KLITZKE, P., MIDTTØMME, K., OLAUSSEN, S., PASCAL, C., RODES, N., SHESTOV, A., SMYRAK-SIKORA, A. and THOMAS, P. J. (2023): The subsurface thermal state of Svalbard and implications for geothermal potential. *Geothermics*, 111: 102702. doi: 10.1016/j.geothermics.2023.102702

SENGER, K., TVERANGER, J., OGATA, K., BRAATHEN, A. and PLANKE, S. (2014): Late Mesozoic magmatism in Svalbard: A review. *Earth-Science Reviews*, 139: 123-144. doi: 10.1016/j.earscirev.2014.09.002

SKJELKVÅLE, B.-L., AMUNDSEN, H. E. F., O'REILLY, S. Y., GRIFFIN, W. L. and GJELSVIK, T. (1989): A primitive alkali basaltic stratovolcano and associated eruptive centres, Northwestern Spitsbergen: Volcanology and tectonic significance. *Journal of Volcanology and Geothermal Research*, 37(1): 1-19. doi: 10.1016/0377-0273(89)90110-8

SMELROR, M., LARSSEN, G. B. (2016): Are there Upper Cretaceous sedimentary rocks preserved on Sørkapp land, Svalbard? *Norwegian Journal of Geology*, 96(2): 147-158. doi: 10.7850/njg96-2-05

SMIRNOV, M. Y., EGBERT, G. D. (2012): Robust principal component analysis of electromagnetic arrays with missing data. *Geophysical Journal International*, 190(3): 1423-1438. doi: 10.1111/j.1365-246X.2012.05569.x

TREIMAN, A. H. (2012): Eruption age of the Sverrefjellet volcano, Spitsbergen Island, Norway. *Polar Research*, 31(17320): 1-7. doi: 10.3402/polar.v31i0.17320

VÅGNES, E., AMUNDSEN, H. E. F. (1993): Late Cenozoic uplift and volcanism on Spitsbergen: Caused by mantle convection? *Geology*, 21(3): 251-254. doi: 10.1130/0091-7613(1993)021<0251:LCUAVO>2.3.CO;2

WILKINSON, M. D., DUMONTIER, M., AALBERSBERG, I. J. *et al.* (2016): The FAIR Guiding Principles for scientific data management and stewardship. *Scientific Data*, 3(1): 1-9. doi: 10.1038/ sdata.2016.18

WORSLEY, D. (2008): The post-Caledonian development of Svalbard and the western Barents Sea. *Polar Research*, 27: 298-317. doi: 10.1111/j.1751-8369.2008.00085.x

Web sources / Other sources (date last accessed: 18.12.2023)

[1] https://vrsvalbard.com/neogene-quaternary-volcanism-and-thermal-springs/
[2] https://www.youtube.com/watch?v=VSVWSe4l9vI
[3] https://www.svalbox.no/map
[4] https://vrsvalbard.com/neogene-quaternary-volcanism-and-thermal-springs/
[5] https://www.vrsvalbard.com
[6] https://www.vrsvalbard.com/map

Table 3. (Supplementary Material): Synthesis of acquired data with key data responsibles.

Data	Location/comment	Number	Key contacts
Digital field data			
Photospheres	Entire study area www.vrsvalbard.com/map	509	Rafael Horota, Kim Senger
Digital outcrop models	Entire study area www.svalbox.no/map	40	Peter Betlem, Kim Senger
Photographs	Entire study area	> 2 000	All participants
Sampling of rocks			
BVC	Sverrefjellet		Anniken Helland-Hansen, Sebastian Tappe, Dmitrii Zastrozhnov
BVC	Halvdanpiggen		Anniken Helland-Hansen, Sebastian Tappe, Dmitrii Zastrozhnov
BVC	Sigurdfjellet		Anniken Helland-Hansen, Sebastian Tappe, Dmitrii Zastrozhnov
Seidfjellet Fm	Scott-Keltiefjellet		Maria Telmon, Sebastian Tappe, Dmitrii Zastrozhnov
Seidfjellet Fm	Lavatoppen		Maria Telmon, Sebastian Tappe, Dmitrii Zastrozhnov
Seidfjellet Fm	Risefjella		Maria Telmon, Sebastian Tappe, Dmitrii Zastrozhnov
Seidfjellet Fm	Prismefjella		Maria Telmon, Sebastian Tappe, Dmitrii Zastrozhnov
Seidfjellet Fm	Prinsetoppen		Maria Telmon, Sebastian Tappe, Dmitrii Zastrozhnov
Magnetic susceptibility	40 (samples) 220 (susceptibility measurements in field)		Agnes Kontny
Noble gas isotopes	10 samples, across the study area		Horst Kämpf, Sebastian Tappe, Agnes Kontny
Water, gas and travertine sampling			
Jotunkjedene	2 water, 3 gas and 5 travertine samples, additional 4 samples of sea water		Horst Kämpf
Trollkjedene	3 water, 3 gas and 6 travertine samples		Horst Kämpf, Sebastian Tappe
Gygrekjelda	1 water and 1 travertine sample, additional 1 sample of glacial melt water		Horst Kämpf
Field parameters	11 (pH, conductivity, T); Table 1, Fig. 5		Horst Kämpf
Miscellaneous sampling			
Woodfjorden, Bockfjorden	8 drift wood and 10 marine biota samples	4 stations	Horst Kämpf
Geophysics			
Magnetotelluric	Woodfjorden, Bockfjorden	12 stations	Aleksander Minakov